2018

Dispersive shock waves governed by the Whitham equation and their stability

Xin An
University of Wollongong, xa989@uowmail.edu.au

Timothy R. Marchant
University of Wollongong, tim@uow.edu.au

Noel F. Smyth
University of Wollongong

Dispersive shock waves governed by the Whitham equation and their stability

Abstract

Dispersive shock waves (DSWs), also termed undular bores in fluid mechanics, governed by the non-local Whitham equation are studied in order to investigate short wavelength effects that lead to peaked and cusped waves within the DSW. This is done by combining the weak nonlinearity of the Korteweg-de Vries equation with full linear dispersion relations. The dispersion relations considered are those for surface gravity waves, the intermediate long wave equation and a model dispersion relation introduced by Whitham to investigate the 120◦ peaked Stokes wave of highest amplitude. A dispersive shock fitting method is used to find the leading (solitary wave) and trailing (linear wave) edges of the DSW. This method is found to produce results in excellent agreement with numerical solutions up until the lead solitary wave of the DSW reaches its highest amplitude. Numerical solutions show that the DSWs for the water wave and Whitham peaking kernels become modulationally unstable and evolve into multi-phase wavetrains after a critical amplitude which is just below the DSW of maximum amplitude.

Disciplines

Engineering | Science and Technology Studies

Publication Details

An, X., Marchant, T. R. & Smyth, N. F. (2018). Dispersive shock waves governed by the Whitham equation and their stability. Proceedings of the Royal Society A: Mathematical, Physical and Engineering Sciences, 474 (2216), 20180278-1-20180278-18.

PROCEEDINGS A

rspa.royalsocietypublishing.org

Research

Article submitted to journal

Subject Areas:
nonlinear waves, fluid mechanics

Keywords:
Dispersive shock waves, Whitham equation, KdV equation, Modulation theory, Solitary waves, Undular bores

Author for correspondence:
T.R. Marchant
e-mail: t.marchant@uow.edu.au

Dispersive shock waves governed by the Whitham equation and their stability

X. An[1], T.R. Marchant[1] and N.F. Smyth[1,2]

[1]School of Mathematics and Applied Statistics, University of Wollongong, Northfields Ave., Wollongong NSW 2522, Australia

[2]School of Mathematics, University of Edinburgh, James Clerk Maxwell Building, The King's Buildings, Peter Guthrie Tait Road, Edinburgh, Scotland, U.K. EH9 3FD

Dispersive shock waves (DSWs), also termed undular bores in fluid mechanics, governed by the nonlocal Whitham equation are studied in order to investigate short wavelength effects that lead to peaked and cusped waves within the DSW. This is done by combining the weak nonlinearity of the Korteweg-de Vries equation with full linear dispersion relations. The dispersion relations considered are those for surface gravity waves, the intermediate long wave equation and a model dispersion relation introduced by Whitham to investigate the 120^o peaked Stokes wave of highest amplitude. A dispersive shock fitting method is used to find the leading (solitary wave) and trailing (linear wave) edges of the DSW. This method is found to produce results in excellent agreement with numerical solutions up until the lead solitary wave of the DSW reaches its highest amplitude. Numerical solutions show that the DSWs for the water wave and Whitham peaking kernels become modulationally unstable and evolve into multi-phase wavetrains after a critical amplitude which is just below the DSW of maximum amplitude.

THE ROYAL SOCIETY PUBLISHING

1. Introduction

A generic and extensively studied solution of nonlinear, dispersive wave equations, such as the Korteweg-de Vries (KdV), the nonlinear Schrödinger and the Sine-Gordon equations, is the solitary wave, or soliton for integrable equations [1]. Another generic solution of such equations is the dispersive shock wave (DSW), also termed an undular bore in fluids contexts or a collisionless shock wave [2]. A DSW is the dispersive resolution of a discontinuity and the equivalent of a shock wave in compressible flow, with dispersion rather than viscosity smoothing the discontinuity. A DSW is a modulated periodic wave which consists of solitary waves at one edge and linear dispersive waves at the opposite edge. It is a non-steady wave, unlike a solitary wave, as the two edges have different velocities and waves are created within the DSW as it expands. For this reason, it has received much less attention and analysis than solitary waves, even though it is very common in nature [2–6].

The study of bores first arose in water wave theory [1,7,8]. Classic examples of a bore are the tidal bores which arise in coastal regions of strong tidal flow, such as the Severn Estuary in England and Bay of Fundy in Canada, and the tsunami which is generated by marine earthquakes and land slips. Bores in fluids can be categorised into two types, viscous and undular bores. Viscous bores arise when there is a balance between viscous loss, nonlinearity and dispersion; such bores are steady waveforms [1,7], and are not the focus of the present work. On the other hand, when viscous effects can be neglected, DSWs or undular bores arise, which, as stated above, are unsteady, continuously spreading waveforms. In the context of fluid flow DSWs arise in the atmosphere, a classic example being "morning glory" waves [3,9,10], in the semi-diurnal internal tide [5] and in transcritical flow over topography [11–14]. In a related geophysical application, DSWs arise in magma flow [4,15,16]. In non-fluids applications, DSWs arise in optics, for example in photorefractive crystals [6,17], nonlinear optical fibres [18,19], nematic liquid crystals [20,21] and colloidal media [22].

As DSWs are unsteady waveforms, their analysis is more challenging than for solitary waves. The key to obtaining DSW solutions was the development of Whitham modulation theory [1,23, 24] (related to the method of multiple scales) for analysing slowly varying, nonlinear, dispersive waves. The Whitham modulation equations form a system of partial differential equations for the slowly varying parameters of a periodic wavetrain, such as amplitude, wavenumber and mean height. If this system is elliptic, the wavetrain is modulationally unstable and if it is hyperbolic, it is modulationally stable. For hyperbolic systems a DSW solution occurs as a simple wave solution of the modulation equations. In particular, Whitham derived the modulation equations for the KdV equation and set them in a simple Riemann invariant form [1,24]. The DSW solution of the KdV equation was subsequently found from these modulation equations [25,26]. Once the connection between DSW solutions and hyperbolic Whitham modulation equations was realised, the DSW solutions of other standard (integrable) nonlinear, dispersive wave equations, such as the NLS [27], the Sine-Gordon [28] and the Gardner equations [29] were found. The key to finding these DSW solutions from modulation equations is the ability to set them in Riemann invariant form, which is possible if the underlying equation is integrable [30].

If the underlying nonlinear dispersive equation is not integrable, then the determination of the Whitham modulation equations and their Riemann invariant form, if hyperbolic, is a non-trivial problem (if the latter is indeed possible for systems of order greater than 2, which is Pfaff's problem). A significant advance in this regard was the realisation that if the DSW is of KdV type and the differential equation determining the periodic wave solution is of the form $u_\theta^2 = r^2(u)P(u)$, where θ is the phase, $P(u)$ is a cubic polynomial and $r(u)$ is some smooth function which does not vanish at the roots of $P(u)$, then the Whitham modulation equations have a simplified, degenerate structure at the two edges of the DSW, the solitary wave and linear wave limits [2,31,32]. The basic assumption is that the periodic wave solution has properties similar to the elliptic function cnoidal wave solutions of the KdV (and NLS) equations. The simplified structure can then be used to determine the leading and trailing edges of the DSW

from the linear dispersion relation alone without knowledge of the full Whitham modulation equations [2,31,32]. This method for non-integrable equations, termed dispersive shock fitting, was then used to determine the leading and trailing edges of DSWs governed by non-integrable equations arising in a number of applications, including fluids, nonlinear optics and Bose-Einstein condensates [2,15,17,22,33,34]. The shock fitting method has recently been extended to nonlinear dispersive wave equations with Benjamin-Ono dispersion, for which the equation governing the periodic wave solution is not of the form $u_\theta^2 = r^2(u)P(u)$, but the DSW is of KdV type [35]. In many observational measurements only the solitary wave edge of a DSW can be fully resolved [5], so the restriction of El's method to the leading and trailing edges of a DSW is not a severe one.

It is well known that water waves peak (and break) when their amplitude to depth ratio is high enough. The nonlinear shallow water equations, which neglect dispersion, show typical hyperbolic breaking [1]. If long wave dispersion is added to the shallow water equations, the Boussinesq and KdV equations arise [1], which possess soliton solutions. However, solutions of these equations show no breaking due the dispersion being too strong for short waves. In addition, Stokes showed that there is a wave of maximum amplitude for steady water waves and that this wave has a sharp peak of angle 120^o [36]. Again, the KdV and Boussinesq equations do not reproduce this behaviour as they possess solutions of arbitrary amplitude. The full water wave peaking is due to short wave effects, beyond the Boussinesq and KdV asymptotic approximations.

To understand the connection between nonlinearity, dispersion, peaking and breaking, Whitham introduced model nonlinear dispersive equations which incorporate KdV type quadratic nonlinearity and full dispersion, in particular full linear water wave dispersion [1,25]. It was found that full water wave dispersion gives rise to a wave of greatest height, but with a cusp, not a sharp peak of 120^o. To understand why the water wave kernel resulted in a wave of greatest height with a cusp and not a peak, Whitham introduced an exponential approximation to the water wave kernel which was found to give a wave of greatest height with a peak of angle 110^o. Whitham also studied other dispersive Fourier kernels which give rise to peaked waves and breaking for sufficiently asymmetric waves [1,37]. These type of nonlinear dispersive equations with KdV nonlinearity and full Fourier dispersion have subsequently been termed Whitham equations and have been found useful to study peaking and breaking effects, present in the full water wave equations, but based on a much simpler model equation [38]. More recent work has shown the existence of travelling and solitary wave solutions of the Whitham equation with various dispersive kernels [38–40]. The dispersion relation in the Whitham equation can also be extended beyond surface water waves to internal waves in a stratified fluid [41].

The present work studies the DSW solution of the Whitham equation for three different linear dispersion relations, for surface water waves on a fluid of finite depth [1], for the intermediate long wave equation for a stratified fluid [41] and a model kernel introduced by Whitham to model wave peaking as for the Stokes wave of greatest amplitude [1]. The shock fitting method [2,31,32] discussed above is used to obtain the leading, solitary wave edge and the trailing, linear wave edge of the DSWs. It is found that the shock fitting method gives results in excellent agreement with numerical solutions for all three dispersion relations. A particular emphasis of the study is the behaviour of the DSW as the leading solitary wave approaches the wave of greatest amplitude. Numerical solutions show that the DSWs for the water wave and peaking kernels then become unstable just below this maximum and evolve into a two phase wavetrain. This cannot be captured with the dispersive shock fitting method as it assumes a single phase wavetrain. The standard shock fitting method assumes that the DSW has the standard KdV type structure, for which certain admissibility criteria need to be satisfied which relate to the genuine nonlinearity and hyperbolicity of the Whitham modulation equations [2,15]. In the shock fitting method, failure of the admissibility conditions is shown by the non-monotonicity of the trailing edge group velocity and the leading edge solitary wave velocity as the levels ahead and behind vary. In particular, loss of hyperbolicity indicates that the bore becomes modulationally unstable, which in numerical solutions typically results in a multi-phase wavetrain appearing in the DSW,

which is what is found here for the Whitham equations for the water wave and peaking kernels. However, while it is found that the admissibility condition for genuine nonlinearity fails at the trailing edge as the initial jump height increases, the breakdown of the DSW is not due to this. It is found from numerical solutions that the instability is generated at the leading, solitary wave edge and propagates back through the DSW. This instability is due to a Benjamin-Feir instability [42] of the periodic wave solution of the Whitham equation as the wavenumber decreases [1,42], which was detailed by Sanford *et al* [43]. It is found that this Benjamin-Feir instability arises just after the breakdown of genuine nonlinearity and dominates it.

2. Whitham equations and dispersion relations

(a) Intermediate long waves

The KdV equation models the propagation of weakly nonlinear long waves at the interface of a two layer fluid in the limit in which the wavelength is much larger than the total depth of the fluids. However, when the lower layer is relatively thick compared with the wavelength, the waves are governed by the intermediate long wave equation [41], which is integrable [44]. This equation was introduced as a model for weakly nonlinear waves much longer than a pycnocline thickness in a stratified fluid of finite total depth. Combining the dispersion of the intermediate long wave equation with quadratic nonlinearity gives the Whitham equation

$$u_t + 2uu_x + i\int_{-\infty}^{\infty} G(x-\xi)u_{\xi\xi}(\xi,t)\,d\xi = 0, \quad G = \mathcal{F}^{-1}\left\{\coth k - \frac{1}{k}\right\}, \tag{2.1}$$

where $\mathcal{F}$ denotes the Fourier transform. This equation has the exact soliton solution [45]

$$u = \beta + \frac{r\sin r}{\cosh(r(x-V_s t)) + \cos r}, \quad V_s = 2\beta + 1 - r\cot r. \tag{2.2}$$

The amplitude of the soliton is then $A_s = r\sin r/(1+\cos r)$, with its velocity V_s implicitly determined from this through the parameter r.

In principle, as the intermediate long wave equation is integrable, its Whitham modulation equations can be determined and set in Riemann invariant form. In the present work, the intermediate long wave equation will be used as an example equation which can be expressed as a Whitham equation, but which does not have a wave of maximum height and which possesses DSWs that are stable.

(b) Water waves

The original Whitham equation [1,25] combined the quadratic nonlinearity of the KdV equation with the full dispersion of gravity waves on a fluid of finite depth. This equation is

$$u_t + 2uu_x - u_x + \int_{-\infty}^{\infty} K(x-\xi)u_\xi(\xi,t)\,d\xi = 0, \quad K = \mathcal{F}^{-1}\left\{\sqrt{\frac{\tanh k}{k}}\right\}. \tag{2.3}$$

where the acceleration due to gravity and depth have been normalised to 1. In the limit of long waves $k \to 0$, the dispersion relation for this equation reduces to $\omega = \sqrt{\tanh k/k} = k - \frac{1}{6}k^3 + \mathcal{O}(k^5)$. This then gives the KdV dispersive term, as required. As noted in the Introduction, this water wave equation gives a wave of greatest height with a cusp [1], rather than the Stokes limiting wave with a peak of angle 120^o [36].

The dispersive shock fitting method provides the velocity of the leading solitary wave of a DSW. To find its corresponding amplitude, the amplitude-velocity relation for a solitary wave needs to be known, but this cannot be found analytically for the water wave Whitham equation (2.3). Hence, its amplitude-velocity relation must be found numerically in order to obtain comparisons with numerical solutions for the leading wave amplitude. In this regard, we seek a

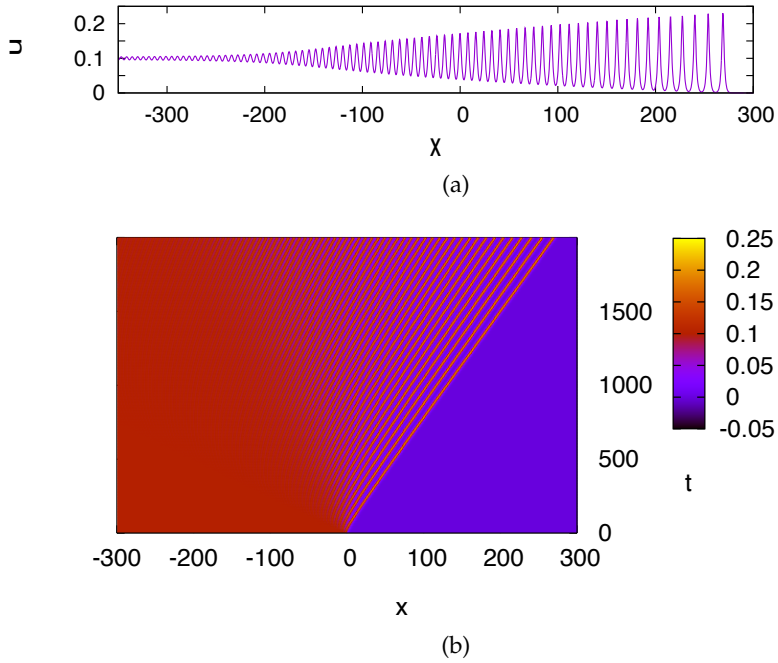

Figure 1: Numerical DSW solution of the Whitham equation for water waves (2.3). The parameters are $u_- = 0.1$ and $u_+ = 0.0$. Shown are (a) the surface profile u versus x at $t = 2000$, (b) contour evolution plot of u in the (x, t) plane.

travelling wave solution $u = f(\theta) = f(x - Vt)$. The water wave equation (2.3) becomes

$$-Vf + f^2 + \int_{-\infty}^{\infty} K(\theta - \xi) f(\xi)\, d\xi = C = -V\beta + \beta^2 + \beta \int_{-\infty}^{\infty} K(\theta - \xi)\, d\xi \tag{2.4}$$

on integrating and assuming that $f \to \beta$ as $|\theta| \to \infty$. It is noted that the boundary value can be taken as $\beta = 0$ as the Whitham equation has the invariance that if the solitary wave solution $f \to \beta$ as $\theta \to \pm\infty$, the transformation $f \to f - \beta$ results in $V \to V + 2\beta$. The steady wave solution equation (2.4) was solved numerically using the spectral method of Ehrnström and Kalisch [38–40], from which numerical amplitude-velocity results can be obtained. The work of Ehrnström and Kalisch [39,40] shows that solitary wave solutions can be obtained by calculating periodic wave solutions and then increasing their wavelength until a solitary wave results.

(c) Peaking model

As noted in the Introduction, the Whitham equation (2.3) does not give the peaked highest wave of Stokes [36], but gives a cusped wave of maximum amplitude instead. To further study the type of dispersive kernel which generates a peaked wave of maximum amplitude, Whitham [1,37] introduced the nonlocal equation

$$u_t + 2uu_x - u_x + \int_{-\infty}^{\infty} L(x - \xi) u_\xi(\xi, t)\, d\xi = 0, \quad L = \mu e^{-\nu|x|}, \quad \mu = \pi/4, \quad \nu = \pi/2. \tag{2.5}$$

Whitham showed that this equation has a peaked highest wave solution of peak angle 110^o. As the Whitham equation (2.5) is just a model, it is not expected that it would reproduce the 120^o Stokes wave. An additional reason for the choice of the dispersive kernel in the Whitham equation

(2.5) is that it is the Green's function for the operator $d^2/dx^2 - \nu^2$, so that it is the solution of

$$\frac{d^2L}{dx^2} - \nu^2 L = -\nu^2\delta(x). \tag{2.6}$$

This enables the solitary wave solution of of the Whitham equation (2.5) to be determined exactly.

The simplest initial condition which will result in the generation of a DSW is the step initial condition

$$u(x,0) = \begin{cases} u_-, & x<0, \\ u_+, & x>0 \end{cases} \tag{2.7}$$

with $u_- > u_+$. The DSW solutions of the Whitham equations (2.1)–(2.5) are of similar appearance and only differ in the details, such as leading wave amplitude and leading and trailing edge velocities, for a given jump $u_- - u_+$. Figure 1 shows a DSW solution for the surface water wave Whitham equation (2.3) for the level ahead $u_+ = 0$ and the level behind $u_- = 0.1$. These initial values mean that the waves of the DSW are far from the maximum amplitude wave. The DSW has a similar appearance to the KdV DSW [25], which is discussed in Section 3(a). The amplitude of the lead solitary wave is 0.23, which is slightly higher than the KdV DSW lead wave amplitude of $2(u_- - u_+) = 0.2$.

3. DSWs for the Whitham equation

As discussed in the Introduction, El [2,31,32] developed the dispersive shock fitting method to determine the details of the leading and trailing edges of a DSW of KdV type. The importance of this method is that it is applicable even when the Whitham modulation equations for the governing nonlinear dispersive wave equation are not known. The shock fitting method is based on the deduction that the leading and trailing edges of a DSW can be determined solely from the non-dispersive form of the equation applying outside of the DSW region and the linear dispersion relation for the equation. The non-dispersive form of all the Whitham equations (2.1)–(2.5) applying outside the DSW are

$$\frac{\partial \bar{u}}{\partial t} + 2\bar{u}\frac{\partial \bar{u}}{\partial x} = 0. \tag{3.1}$$

The notation $\bar{u}$ is used for the non-dispersive region as the solution in the non-dispersive region matches with the mean of u at the edges of the DSW [2,31,32]. The characteristic velocity of the non-dispersive equation is then $V(\bar{u}) = 2\bar{u}$.

El [2,31,32] showed that matching between the non-dispersive region behind the DSW and the trailing edge of the DSW gives that the wavenumber k at the trailing edge of the DSW is determined by

$$\frac{dk}{d\bar{u}} = \frac{\frac{\partial \omega}{\partial \bar{u}}}{V(\bar{u}) - \frac{\partial \omega}{\partial k}}, \tag{3.2}$$

with $\omega = \omega(\bar{u}, k)$ the linear dispersion relation and $\bar{u}$ the mean of u in the DSW. The boundary condition for this differential equation is $k(u_+) = 0$, which links the trailing edge to the leading, solitary wave edge of the DSW where the wavenumber vanishes. The position of the trailing edge of the DSW is then determined from the group velocity

$$s_- = \frac{\partial \omega(u_-, k_-)}{\partial k} \tag{3.3}$$

at the trailing edge.

The leading, solitary wave edge of the DSW is determined in a similar fashion, but in terms of "conjugate" variables. The "conjugate frequency" $\widetilde{\omega}$ is given in terms of the "conjugate wavenumber" $\widetilde{k}$ by $\widetilde{\omega} = -i\omega(\bar{u}, i\widetilde{k})$. Then, as for the linear wave edge, the leading, solitary wave

edge of the DSW is determined by

$$\frac{d\widetilde{k}}{d\overline{u}} = \frac{\frac{\partial\widetilde{\omega}}{\partial\overline{u}}}{V(\overline{u}) - \frac{\partial\widetilde{\omega}}{\partial\widetilde{k}}}, \tag{3.4}$$

with the boundary condition $\widetilde{k}(u_-) = 0$ to link to the trailing, linear edge. The position of the leading edge of the DSW is thus given by its velocity s_+, with

$$s_+ = \frac{\widetilde{\omega}(u_+, \widetilde{k}_+)}{\widetilde{k}_+}. \tag{3.5}$$

Modulation theory gives that this is the same as the solitary wave velocity V_s, so that $s_+ = V_s$. The reason for the use of these complex "conjugate" variables is due to the underlying assumption of the dispersive shock fitting method that the periodic wave solution is given by $u_\theta^2 = r^2(u)P(u)$, where $P(u)$ is a cubic polynomial and $r(u)$ is some smooth function which does not vanish at the roots of $P(u)$. This then connects the periodic wave solution to elliptic functions, so that the solitary wave solution in the real direction is connected to a "conjugate" (linear) periodic wave in the imaginary direction.

In Section 5 the details of the leading and trailing edges of the DSWs for the Whitham equations (2.1)–(2.5) will be compared with their equivalents for the KdV equation, which is (2.3) with $K = 1 + \frac{1}{6}\partial^2/\partial x^2$. The velocity s_- of the trailing edge and the amplitude A_s and velocity $s_+ = V_s$ of the leading edge of the KdV DSW are [25,26]

$$s_- = 4u_+ - 2u_-, \quad s_+ = V_s = \frac{2}{3}u_+ + \frac{4}{3}u_-, \quad A_s = \frac{3}{2}s_+ - 3u_+ = 2\left(u_- - u_+\right). \tag{3.6}$$

With these preliminaries, the leading and trailing edges of the DSWs for the Whitham equations (2.1)–(2.5) can be determined.

(a) Intermediate long wave DSW

The linear dispersion relation for the intermediate long wave Whitham equation (2.1) is

$$\omega = 2\overline{u}k - k^2\coth k + k. \tag{3.7}$$

The trailing, linear wave edge of the DSW is then determined by the differential equation (3.2) with the boundary condition $k(u_+) = 0$ to match with the leading edge. Solving this equation gives

$$\frac{1}{2}\ln\frac{e^{2k}-1}{k} + \frac{k}{e^{2k}-1} = \bar{u} - u_+ + \ln\sqrt{2} + \frac{1}{2}. \tag{3.8}$$

Then at the trailing, linear edge $k = k_-$ and $u = u_-$. The velocity s_- of the trailing edge is the linear group velocity

$$s_- = \frac{\partial\omega}{\partial k} = 2u_- + k_-^2\coth^2 k_- - 2k_-\coth k_- - k_-^2 + 1 \tag{3.9}$$

with k_- the solution of (3.8) with $k = k_-$ and $\bar{u} = u_-$.

The leading, solitary wave edge is determined in a similar fashion from the conjugate equation (3.4) with the condition $\widetilde{k}(u_-) = 0$ linking to the trailing edge. Solving this differential equation gives that the conjugate wavenumber $\widetilde{k} = \widetilde{k}_+$ at the leading edge is the solution of

$$\widetilde{k}_+\cot\widetilde{k}_+ + \ln\frac{\sin\widetilde{k}_+}{\widetilde{k}_+} = -2\left(u_- - u_+\right) + 1. \tag{3.10}$$

With this solution, the velocity of the leading edge of the DSW is the solitary wave velocity

$$s_+ = V_s = \frac{\widetilde{\omega}(u_+, \widetilde{k}_+)}{\widetilde{k}_+} = 2u_+ - \widetilde{k}_+\cot\left(\widetilde{k}_+\right) + 1. \tag{3.11}$$

The amplitude A_s of the leading edge of the DSW is then determined from the intermediate long wave soliton solution (2.2).

(b) Water wave DSW

The linear dispersion relation for the Whitham equation (2.3) with water wave dispersion is

$$\omega = 2\overline{u}k + \sqrt{k\tanh k} - k. \tag{3.12}$$

The differential equation (3.2) for the DSW trailing edge cannot be solved analytically with this dispersion relation, so it will be solved numerically. The velocity of the trailing edge of the DSW is then the group velocity

$$s_- = \frac{\partial\omega(u_-,k_-)}{\partial k} = 2u_- + \frac{1}{2}\frac{\tanh(k_-) + k_-\,\mathrm{sech}^2(k_-)}{\sqrt{k_-\tanh(k_-)}} - 1. \tag{3.13}$$

The solitary wave edge of the DSW is determined in a similar fashion using the conjugate equation (3.4). As for the linear edge, this equation cannot be solved analytically and its solution is found numerically with the condition $\widetilde{k}(u_-) = 0$ to connect the solitary wave edge of the DSW to the linear wave edge. The velocity of the leading edge of the DSW is then the solitary wave velocity

$$s_+ = V_s = \frac{\widetilde{\omega}(u_+,\widetilde{k}_+)}{\widetilde{k}_+} = 2u_+ + \sqrt{\frac{\tan(\widetilde{k}_+)}{\widetilde{k}_+}} - 1. \tag{3.14}$$

As there is no known solitary wave solution of the Whitham equation (2.3), its amplitude-velocity relation will be determined from numerical solitary wave solutions, as outlined in Section 2(b).

The jump height $\Delta = u_- - u_+$ at which the lead wave of the water wave DSW first forms a cusp can be obtained from numerical solutions of the solitary wave equation (2.4). For given u_- and u_+ the velocity $V = s_+$ is obtained from the shock fitting expression (3.14). This velocity is then used in the solitary wave equation (2.4). The jump height is increased until the numerical scheme ceases to converge. In this manner it is found that the DSW reaches maximum amplitude and forms a cusp when $\Delta = 0.162$.

(c) Peaking DSW

The final DSW to be determined is that for the model Whitham equation (2.5) which has a peaked wave of maximum amplitude. The linear dispersion relation for this equation is

$$\omega = 2\overline{u}k + k\left(\frac{2\mu\nu}{k^2+\nu^2} - 1\right). \tag{3.15}$$

As for the intermediate long wave example of Section 3(a), the trailing edge equation (3.2) is solved using this dispersion relation and the matching condition $k(u_+) = 0$ at the leading edge. It is then found that the wavenumber at the trailing edge is the solution of

$$\frac{\mu\ln(k_-^2+\nu^2)}{\nu} - \frac{2\mu\nu}{k_-^2+\nu^2} = 2(u_- - u_+) + \ln\left(\frac{\pi}{2}\right) - 1, \tag{3.16}$$

on setting $k = k_-$ and $\bar{u} = u_-$ in the solution. The velocity of the linear wave edge is then the group velocity

$$s_- = \frac{\partial\omega(u_-,k_-)}{\partial k} = 2u_- + \frac{2\mu\nu}{k_-^2+\nu^2} - 1 - \frac{4k_-^2\mu\nu}{(k_-^2+\nu^2)^2}. \tag{3.17}$$

The leading, solitary wave edge of the DSW is determined in a similar fashion. Solving the conjugate equation (3.2) gives that the conjugate wavenumber $\widetilde{k}_+$ at the leading edge is the

solution of

$$\frac{1}{4}\ln\left(\frac{\nu^2-\widetilde{k}_+^2}{\nu^2}\right)+\frac{1}{2}\left(\frac{2\mu\nu}{\widetilde{k}_+^2-\nu^2}+1\right)=u_+-u_-. \tag{3.18}$$

The velocity of the leading edge of the DSW is thus the solitary wave velocity

$$s_+=V_s=\frac{\widetilde{\omega}_s(u_+,\tilde{k}_+)}{\widetilde{k}_+}=2u_++\frac{2\mu\nu}{\nu^2-\tilde{k}_+^2}-1. \tag{3.19}$$

For this peaked wave case the amplitude-velocity relation can be determined analytically as the dispersive kernel of the Whitham equation (2.5) is the solution of the ordinary differential equation (2.6).

We seek a solitary wave solution of the Whitham equation (2.5) of the form $u=f(x-Vt)=f(\theta)$. Substituting this travelling wave form into the equation and integrating once gives

$$-Vf+f^2-f+\int_{-\infty}^{\infty}L(\theta-\xi)f(\xi)\,d\xi-C_1=0, \tag{3.20}$$

where C_1 is a constant of integration. We now use that L is the solution of (2.6), so that

$$\left(\partial_\theta^2-\nu^2\right)\left[(V+1)f-f^2\right]+\nu^2\left(f-C_1\right)=0. \tag{3.21}$$

Multiplying (3.21) by $\partial_\theta\left((V+1)f-f^2\right)=(V+1-2f)f'$ and integrating with respect to θ gives

$$\begin{aligned}&\left[(V+1)-2f\right]^2f'^2-\nu^2\left\{\left[(V+1)f-f^2\right]^2-(V+1)f^2+\frac{4}{3}f^3\right\}\\&+2\nu^2C_1\left[f^2-(V+1)f\right]=C_2,\end{aligned} \tag{3.22}$$

where C_2 is another constant of integration. The constants of integration can be found on assuming that the solitary wave is on a constant background, so that $f\to\beta$ and $f'\to0$ as $\theta\to\pm\infty$. Thus, we obtain

$$C_1=-V\beta+\beta^2,\quad C_2=\nu^2\left\{\left[(V+1)\beta-\beta^2\right]^2+(V+1)\beta^2-\frac{4}{3}\beta^3\right\}. \tag{3.23}$$

At the solitary wave maximum, $f=f_m$ and $f'=0$. We then obtain from the differential equation (3.22) and the expressions (3.23) for the constants of integration that the solitary wave velocity is the solution of the quadratic

$$(V+1)^2-(1+2f_m+2\beta)(V+1)+(f_m+\beta)^2+\frac{4}{3}f_m+\frac{2}{3}\beta=0. \tag{3.24}$$

The positive square root of this quadratic is chosen to give the correct velocity as $f_m\to\beta$, so that

$$V+1=\frac{1}{2}\left\{1+2f_m+2\beta+\sqrt{1-\frac{4}{3}(f_m-\beta)}\right\}. \tag{3.25}$$

As shown by Whitham [1], equation (3.22) governing the periodic wave solution gives that peaking occurs when $V+1=2f_p$, where f_p denotes the peak height. By setting $f_m=f_p$ the amplitude-velocity relation (3.25) then gives the peak amplitude, the rise at the peak above the background β, as $A_p=f_p-\beta$. The velocity expression (3.25) thus gives that peaking occurs when $f_m-\beta=2/3$, so that the lead wave velocity (3.19) gives the limiting conjugate wavenumber $\widetilde{k}_p=\pi/4$. The critical jump height at which the lead wave of the DSW peaks is then given by (3.18) as $\Delta=u_--u_+=1/6-\ln(3/4)/4\approx0.239$.

4. DSW breakdown

As the height $\Delta=u_--u_+$ of the initial jump (2.7) grows, the amplitude of the lead solitary waves of the DSWs increase for the Whitham equations with the water wave and peaking kernels

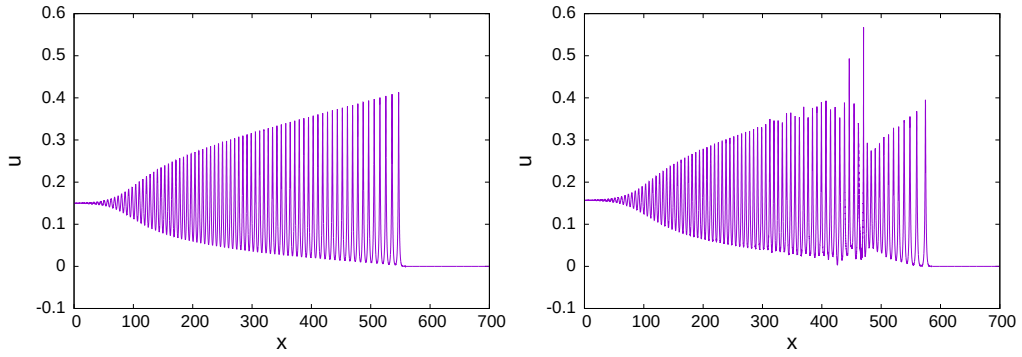

(a) (b)

Figure 2: DSW stability threshold. Numerical solutions of the Whitham equation with the water wave kernel (2.3) for the initial condition (2.7). (a) below threshold $u_- = 0.15$; (b) above threshold $u_- = 0.157$. The level ahead is $u_+ = 0$ and $t = 3000$.

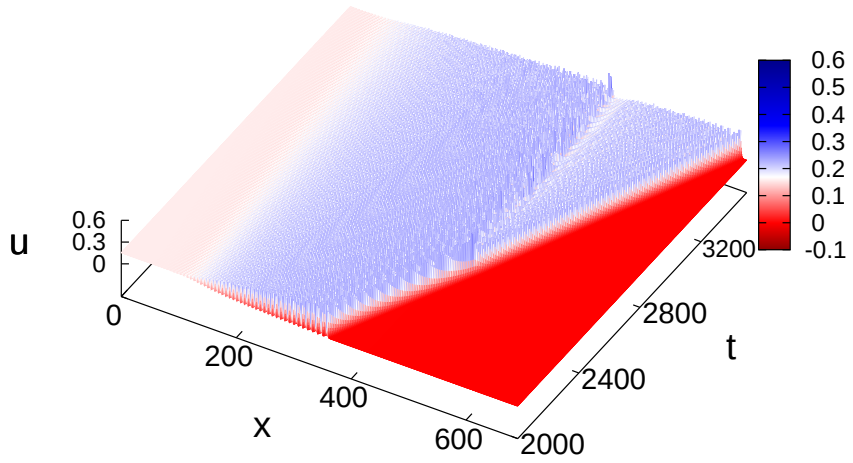

Figure 3: DSW instability. Numerical solutions for the evolution of an unstable DSW governed by the Whitham equation with the water wave kernel (2.3) for the initial condition (2.7). Evolution around onset of instability. The parameter values are $u_- = 0.157$ and $u_+ = 0$.

until they reach a maximum. The lead wave of the water wave DSW first has a cusp at $\Delta \approx 0.162$. This results in the leading edge of the DSW becoming flat as the maximum wave is appoached as the jump height increases. The resulting DSW appears similar to a DSW propagating in water of decreasing depth [46]. In this case, the shoaling of the DSW causes it to eject a train of solitary waves ahead of it, due to mass conservation. While the DSWs have similar appearance, the cause is different here as the approach to a maximum wave causes the levelling of the leading edge of DSWs in the present work.

Numerical results show that when $\Delta = 0.152$, the water wave DSW becomes unstable. For higher jump heights, the lead solitary wave of the DSW develops an instability, which propagates back through it, resulting in the DSW becoming a multiphase wavetrain. The development of this instability is illustrated in Figures 2 and 3. The numerical DSW solution shown in Figure 2(a) is just below the threshold, with $\Delta = 0.15$. The DSW has the standard KdV form, with some flattening of the leading wave amplitude due to these waves approaching the limiting wave form. An unstable DSW just above the threshold, with $\Delta = 0.157$, is illustrated in Figure 2(b) with the generation of a multi-phase wavetrain is clearly seen. with the instability arising at around $t = 1500$. The detailed evolution of the instability is shown in Figure 3 for $\Delta = 0.157$. It can be seen from this figure that the instability first occurs at the leading edge of the DSW at around $t = 2500$ and propagates back through it. It will now be shown that this behaviour is due to the modulational instability of the periodic wave solution of the Whitham equation. The Whitham equation with the peaking kernel (2.5) shows similar instability behaviour, with the threshold jump height $\Delta = 0.234$ for the onset of the instability, again slightly lower than the critical jump height $\Delta = 0.239$.

(a) Admissibility conditions

The DSW fitting method is based on the DSW being of KdV type. To ensure this, various admissibility conditions need to be satisfied [2,15]. These relate to the genuine nonlinearity and hyperbolicity of the Whitham modulation equations governing the DSW. The breakdown of these conditions can lead to linear degeneracy and modulational instability due to zero dispersion. In detail, we require that

$$\frac{d}{du_-}s_-(u_-) \neq 0, \quad \frac{d}{du_+}s_-(u_+) \neq 0, \quad \frac{d}{du_-}s_+(u_-) \neq 0, \quad \frac{d}{du_+}s_+(u_+) \neq 0 \tag{4.1}$$

for the shock fitting method to be valid. The first and third criteria imply that the Whitham modulation equations form a genuinely nonlinear system at the linear and solitary wave edges of the DSW, respectively. The breakdown of either of these two conditions means that a centred simple wave solution of the modulation equations, corresponding to a DSW, is not possible. The second and fourth criteria mean that the Whitham modulation equations are strictly hyperbolic at the linear and solitary wave edges of the DSW, respectively. The breakdown of either of these conditions means that there is zero dispersion and the DSW is not modulationally stable. A gradient catastrophe occurs, resulting in compression and implosion of the DSW. The numerical solutions displayed in Figures 2(b) and 3 seem to show modulational instability due to zero dispersion. However, the breakdown of the DSW is more involved than this.

The validity of the admissibility conditions (4.1) can be checked using the leading and trailing edge DSW solutions of Section 3. Differentiating the trailing edge velocity (3.9) and leading edge velocity s_+ (3.11) with respect to u_- and u_+ for the intermediate long wave Whitham equation (2.1), it is found that the admissibility conditions are always satisfied, so that the DSW solution of Section 4 is valid for any jump height $\Delta = u_- - u_+$. Numerical solutions of the intermediate long wave equation (2.1) do not show any instability of the DSW, as is expected as the intermediate long wave equation is integrable.

For the case of the water wave DSW, the derivative ds_-/du_- vanishes when $k = 1.29$, at which wavenumber the jump height is $\Delta = 0.148$. The other derivatives in the admissibility conditions (4.1) do not vanish. The modulation equations then have a breakdown of genuine nonlinearity at the trailing edge for sufficiently large initial jumps. As stated above, the lead wave of the DSW first reaches the maximum amplitude for a jump height $\Delta = 0.162$, so the loss of genuine nonlinearity occurs just below this maximum wave amplitude. However, the numerical solutions displayed in Figures 2(b) and 3 are more indicative of modulation instability, with the generation of a multiphase wavetrain [2]. The resolution of this is found from the stability of the periodic wavetrain for the Whitham equation with the water wave kernel [43]. This work found that the periodic wave solution undergoes Benjamin-Feir instability when its amplitude

is sufficiently large. Rescaling their results to the present form (2.3) of the Whitham equation, this critical amplitude is 0.39, which compares favourably with the lead wave amplitude 0.439 for the jump height $\Delta = 0.151$ just before the DSW becomes unstable, found from numerical solutions. In addition, shock fitting gives the wavenumber $k_- = 1.31$ at the trailing edge for $\Delta = 0.152$, which is very close to the stability boundary for Benjamin-Feir instability for Stokes water waves on water of finite depth $k = 1.36$ [1]. The wavenumber at the instability around $x = 500$ in Figure 2(b) is centred around 0.962, which again is just in the Benjamin-Feir instability region for weakly nonlinear water waves. The water wave DSW then becomes unstable due to Benjamin-Feir instability of the underlying periodic wavetrain solution. The jump height for the onset of instability is just above that for the loss of genuine nonlinearity, so that the Benjamin-Feir instability dominates the effects of loss of genuine nonlinearity in the numerical solutions.

The DSW for the Whitham equation with the peaking kernel, (2.5), shows similar instability behaviour as for the water wave Whitham equation. This is not unexpected as the peaking kernel was introduced as an approximation to the water wave kernel so that the limiting wave had a peak, rather than a cusp, which matches the limiting Stokes water wave [1]. Again, the derivative ds_-/du_- vanishes, this time for the wavenumber $k = 1.070$ for the jump height $\Delta = 0.254$, so that there is a loss of genuine nonlinearity. In addition, $ds_-/du_+ = 0$ when $k = 2.721$, for which $\Delta = 0.721$. However, the leading wave of the DSW peaks at the jump height $\Delta = 0.239$. Hence, in contrast to the water wave kernel, the breaking of the admissibility conditions (4.1) is not relevant for the peaking kernel. However, similar to the water wave kernel, the leading wave of the DSW becomes unstable at the jump height $\Delta = 0.234$ for which the lead solitary wave has amplitude 0.66, again due to modulational instability of the underlying periodic wave. The instability then propagates through the DSW, generating a multiphase wavetrain. The solution in this case is similar to those displayed in Figures 2(b) and 3.

5. Comparisons with numerical solutions

Numerical solutions of the Whitham equations (2.1), (2.3) and (2.5) with the jump initial condition (2.7) will be compared with the DSW modulation solutions of the three Whitham equation variants and also KdV theory. The numerical solutions were obtained using a hybrid spectral method detailed in [39]. The dispersive terms were calculated using fast Fourier transforms and then propagated forward in time using the 4th order Runge-Kutta scheme. To obtain accurate results for initial jumps producing DSWs whose leading edge wave is near the wave of maximum height the time step was halved and the number of Fourier modes doubled until there was no change in the solution to the accuracy reported here. For the numerical calculations, the time step used was $\Delta t = 0.025$ and the number of points was $N = 2^{18}$. Also, the initial condition (2.7) was smoothed using the hyperbolic tangent.

Figure 4 shows comparisons for the lead solitary wave velocity s_+, lead solitary wave amplitude A_s and trailing edge velocity s_- versus the level ahead u_+ for the intermediate long wave equation (2.1). Shown are results from full numerical solutions and the modulation theory of Section 3 for the amplitude and velocity of the leading, solitary wave edge of the DSW and the group velocity of the trailing, linear wave edge. In addition, the figure shows the equivalent results for the KdV DSW (3.6), as the intermediate long wave equation reduces to the KdV equation in the limit of small amplitudes. The level behind $u_- = 1$ is kept fixed as the level ahead u_+ is varied. Figure 4(a) shows this comparison for the velocity s_+ of the lead solitary wave of the DSW. It can be seen that dispersive shock fitting gives leading edge velocities in near perfect agreement with numerical values, with a difference of less than 1%. As expected, the leading edge velocity of the equivalent KdV DSW converges to the Whitham equation value as the jump height $u_- - u_+$ decreases and the wave amplitudes become small. In the KdV limit the solitary wave amplitude has the exact value $2(u_- - u_+)$, which is twice the jump height. However, the KdV velocity differs from the numerical velocity by less than 5% over the entire jump range. Similar conclusions can be made for the leading solitary wave amplitude A_s comparison shown in Figure 4(b). The numerical amplitude and shock fitting amplitude are in excellent agreement

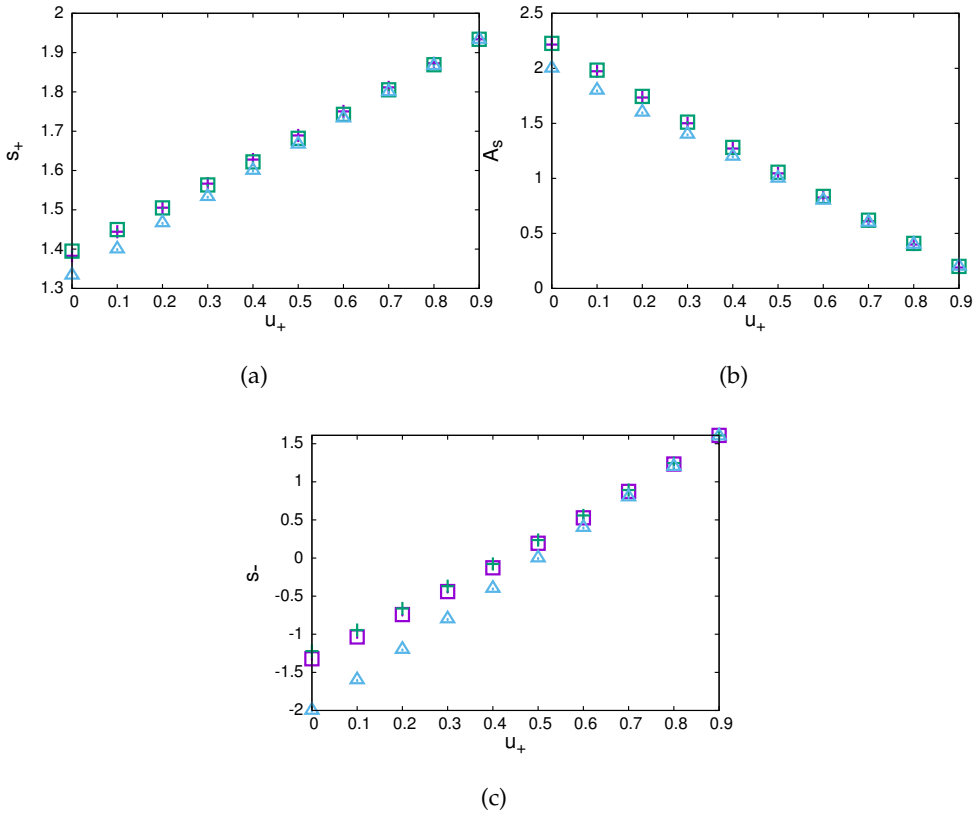

Figure 4: Comparisons between dispersive shock fitting solutions and numerical solutions for intermediate long wave equation (2.1). (a) front velocity s_+, (b) front amplitude A_s, (c) trailing edge velocity s_-. Here $u_- = 1.0$. Numerical solution: (green) $+$; modulation solution (3.11): (purple) $\square$; modulation theory (3.6) for KdV equation: (blue) $\triangle$.

and the KdV modulation theory amplitude converges to these in the limit of a small initial jump. The modulation theory results for the intermediate long wave equation differ by less than 1% from the numerical values, while the KdV modulation theory differs by up to 9%.

The final comparison of Figure 4 is that of Figure 4(c) for the velocity s_- of the trailing, linear edge of the DSW. The agreement between the dispersive shock fitting results and the numerical values, while still very good, is slightly worse than for the leading edge, but with the largest difference still less than 8%. In addition, the KdV trailing edge velocity converges to the Whitham equation value as the jump height decreases, as expected. The major result is that the discrepancy for the KdV trailing edge velocity is much larger than for the leading edge amplitude and velocity, with the difference up to 50%, showing the importance of higher order dispersion on the linear group velocity. In addition, the agreement of the dispersive shock fitting velocity, while very good, is slightly worse than for the leading edge amplitude and velocity. The reason for the poorer agreement between the shock fitting and numerical trailing edge velocities is that the trailing edge position is less certain than the leading edge one as there is no sharp rear edge to the numerical DSW, as can be seen from Figure 1. There is no distinct trailing edge, but a long tail of waves of nearly equal amplitude. Modulation theory predicts that the amplitudes of the waves in the rear of the DSW decrease linearly [1,25,26]. The numerical trailing edge position can then be estimated by linear extrapolation of the rear crests of the DSW down to the level u_- behind [47]. The crests chosen are the distinct, moderate amplitude waves of decreasing amplitude before the long train

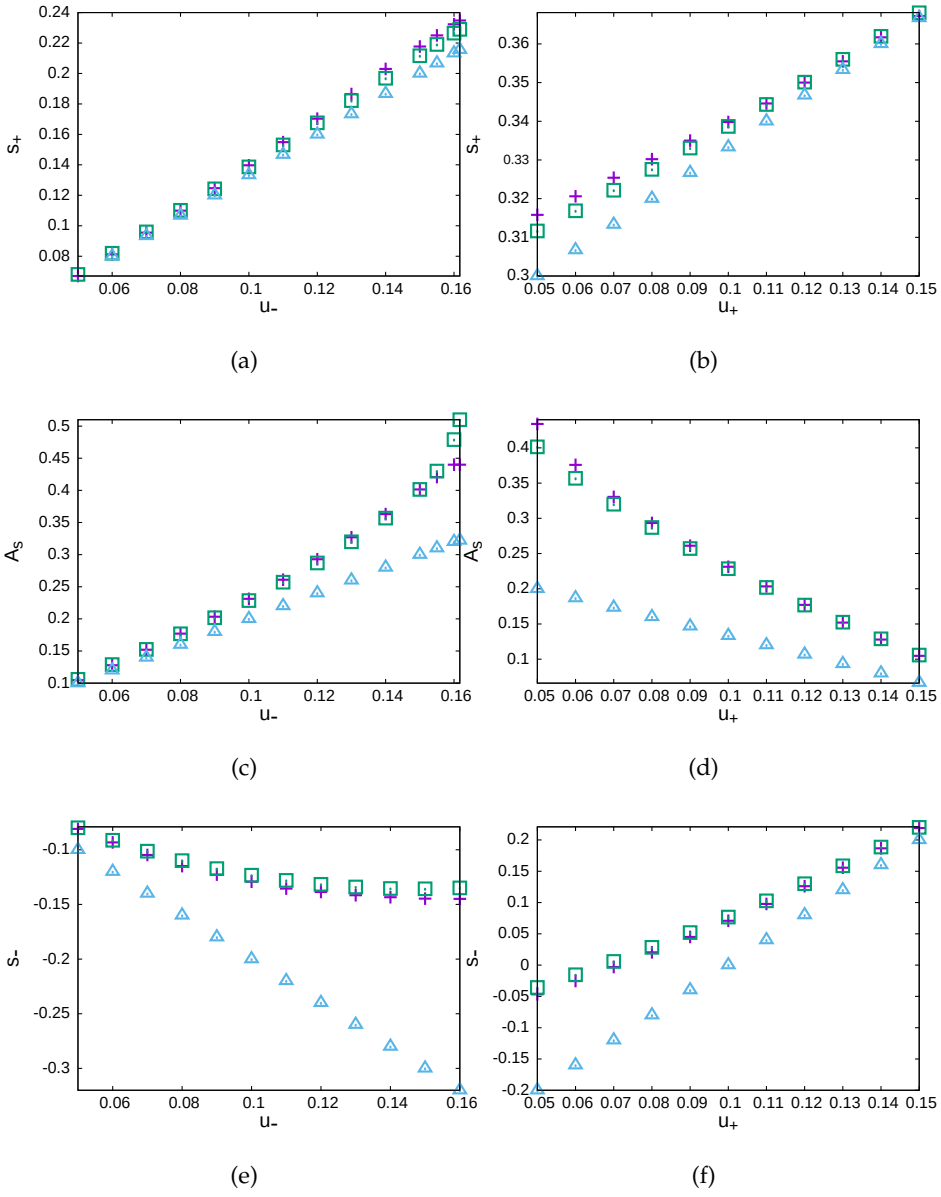

Figure 5: Comparisons between dispersive shock fitting solutions and numerical solutions for the water wave equation (2.3). (a) and (b) front velocity s_+, (c) and (d) front amplitude A_s, (e) and (f) trailing edge velocity s_-. For (a), (c) and (e) $u_+ = 0.0$. For (b), (d) and (f) $u_- = 0.2$. Numerical solution: (purple) $+$; shock fitting solution (3.14) and (2.4): (green) $\square$; DSW modulation solution (3.6) for KdV equation: (blue) $\triangle$.

nearly uniform, small amplitude waves seen in Figure 1a This process is still arbitrary to some extent, which explains the increased difference between the shock fitting and numerical values.

Figure 5 shows comparisons for the lead solitary wave velocity s_+, lead solitary wave amplitude A_s and the trailing edge velocity s_- versus u_- and u_+ for the Whitham equation with the water wave kernel (2.3). This figure has additional comparisons for which the level behind u_- varies, due to the breakdown of the admissibility conditions and instability discussed above. The

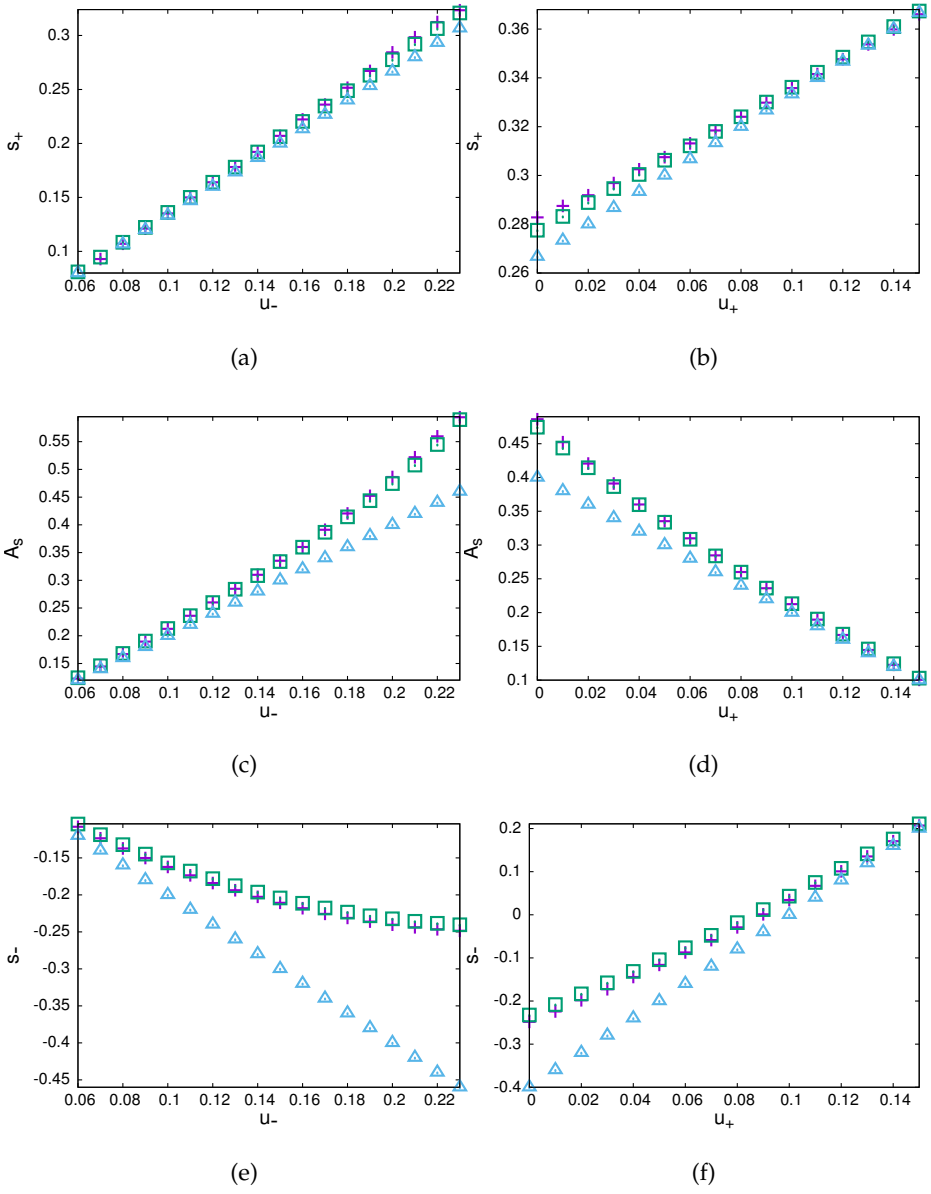

Figure 6: Comparisons between dispersive shock fitting solutions and numerical solutions for peaking equation (2.5). (a) and (b) front velocity s_+, (c) and (d) front amplitude A_s, (e) and (f) trailing edge velocity s_-. For (a), (c) and (e) $u_+ = 0.0$. For (b), (d) and (f) $u_- = 0.2$. Numerical solution: (purple) $+$; shock fitting theory (3.19) and (3.25): (green) $\square$; DSW modulation solution (3.6) for KdV equation: (blue) $\triangle$.

numerical results in this figure are presented beyond the instability threshold at $\Delta = 0.151$. The DSW leading and trailing edges reach an approximate steady state before instability develops, so doing this provides a meaningful comparison. The agreement between the numerical and shock fitting values for the lead solitary wave amplitude and the velocities of the lead solitary wave and trailing, linear edge of the DSW are very good, as for the intermediate long wave equation, except for larger jumps. While the lead wave and trailing wave velocities are in good agreement

for the larger jump heights, the lead wave amplitude shows increasing disagreement. Figures 5(c) and (d) were calculated from the numerical solitary wave amplitude-velocity relation based on equation (2.4) governing a solitary wave. However, the difference is no more than 13%. In detail, the differences between modulation theory and the numerical values of the lead wave and trailing wave velocities and the lead wave amplitude are no more than 3%, 7% and 9%, respectively. Again, the KdV DSW solution shows increasing disagreement as the jump height grows, with the differences with the numerical results increasing to 8%, 58% and 27% for the lead wave amplitude and velocity and the trailing edge velocity, respectively. The reason for the difference between shock fitting and numerical results can be understood from the evolution of the DSW as the maximum amplitude is approached, shown in Figure 2(a). The numerical lead wave amplitude shown in Figure 5(c) levels off as the maximum amplitude is approached, but the shock fitting amplitude shows rapid growth. Dispersive shock fitting gives accurate predictions for the leading and trailing velocities of the DSW, even up to instability. On the other hand, while KdV modulation theory for the lead wave velocity is quite close to the numerical and shock fitting values, even up to instability, this is not the case for the lead wave amplitude and trailing edge velocity. In particular, the KdV trailing edge velocity is far from the numerical values. The KdV velocity linearly decreases, while the numerical and shock fitting values have a slowing rate of decrease. The higher wave frequencies which are incorporated in the Whitham equation, but not asymptotically incorporated in the KdV equation, then have a major role in the DSW evolution.

Figure 6 shows comparisons for the lead solitary wave velocity s_+, lead solitary wave amplitude A_s and the trailing edge velocity s_- versus the level behind u_- (the level ahead is fixed at $u_+ = 0.0$) and the level ahead u_+ (the level behind is fixed at $u_- = 0.2$) for the peaking wave Whitham equation (2.5). In general, the agreement between the numerical solution and the dispersive shock fitting results for the lead solitary wave amplitude and velocity and the trailing edge group velocity is excellent up until the DSW becomes unstable for large jump heights, at which point the numerical values terminate. The dispersive shock fitting results continue past this point, but these cease to be relevant. The peaking condition of Whitham [1], see Section 3(c), gives that the DSW peaks at $u_- = 0.239$. This value was obtained by assuming a zero background depth in equation (3.22), as the initial condition has $u_+ = 0$ for Figure 6. The peak wave is determined by $f' \to +\infty$ at the peak. As for the lead wave velocity for the water wave Whitham equation (2.3), shown in Figures 5(a) and (b), the KdV modulation theory lead wave velocity shown in Figures 6(a) and (b) is again in quite good agreement with the numerical values. However, this is not true for the lead wave amplitude shown in Figures 6(c) and (d) and the trailing edge velocity shown in Figures 6(e) and (f). This is emphasised for the trailing edge velocity as the Whitham equation velocity levels off, while the KdV velocity linearly decreases. Overall, the comparisons of Figure 6 are similar to those for the water wave Whitham equation of Figure 5, which is expected as Whitham introduced the model equation (2.5) to mimic the properties of the full water wave equation (2.3), but to be analytically more tractable, and to produce a highest wave with a sharp peaked crest, as for the full water wave equations, rather than a cusp, as for (2.3) [1]. The differences between the modulation theory results and the numerical values for the lead wave velocity, trailing edge velocity and lead wave amplitude are no more than 2%, 3% and 2%, respectively. On the other hand, the same results for the KdV DSW modulation solution differ from the numerical values by up to 8%, 48% and 28% for the lead wave velocity, the trailing edge velocity and the lead wave amplitude.

6. Conclusions

The dispersive shock wave fitting method [2,31,32] has been used to find the properties of the leading and trailing edges of DSWs governed by the Whitham equation [1] with various dispersion relations (kernels). The Whitham equation is a model equation used to incorporate short wave effects not present in long wavelength, weakly nonlinear expansions of the water wave equations, such as the KdV equation. This is done by incorporating the weak nonlinearity of the KdV equation with the full water wave dispersion via a nonlocal Fourier integral term with

a kernel based on the full dispersion relation. It is found that the shock fitting method again gives results in excellent agreement with full numerical solutions for the leading and trailing edges of a DSW. The results further emphasise the importance of higher frequencies in the evolution of water waves as their amplitudes increase, leading to peaking and other effects. These lead to the amplitudes of the waves in the DSW, particularly at the leading edge, to asymptote to a constant, in sharp contrast to a KdV DSW. The DSW then develops a series of equal amplitude waves at its leading edge. As the level of the initial jump $\Delta = u_- - u_+$ rises, the DSW for the water wave and peaking Whitham equations becomes unstable due to a Benjamin-Feir instability of the underlying periodic wavetrain. This manifests itself by the lead solitary wave becoming unstable. The instability then propagates back through the DSW, generating a multiphase wavetrain. For these equations, the DSWs also violate some of the admissibility conditions for the shock fitting method to be valid. However, these violations either occur for large jump heights which are not relevant, or occur for jump heights just below the instability threshold, so that they do not manifest themselves.

The authors acknowledge their gratitude to the referees for their insightful comments and suggestions for extensions and improvements which have greatly improved this paper and its presentation.

Data Accessibility. This paper has no additional data.

Authors' Contributions. This work was carried out jointly by the authors. XA performed the numerical calculations.

Competing Interests. The authors have no competing interests.

Funding. None.

References

1. G.B. Whitham, 1974, *Linear and Nonlinear Waves,* J. Wiley and Sons, New York.
2. G.A. El and M.A. Hoefer, 2016, "Dispersive shock waves and modulation theory," *Physica D,* **333**, 11–65.
3. R.H. Clarke, R.K. Smith and D.G. Reid, 1981, "The morning glory of the Gulf of Carpentaria: an atmospheric undular bore," *Monthly Weather Rev.,* **109**, 1725–1750.
4. D.R. Scott and D.J. Stevenson, 1984, "Magma solitons," *Geophys. Res. Lett.,* **11**, 1161–1164.
5. N.F. Smyth and P.E. Holloway, 1988, "Hydraulic jump and undular bore formation on a shelf break," *J. Phys. Ocean.,* **18**, 947–962.
6. W. Wan, S. Jia and J.W. Fleischer, 2007, "Dispersive superfluid-like shock waves in nonlinear optics," *Nature Phys.,* **3**, 46–51.
7. R.S. Johnson, 1970, "A non-linear equation incorporating damping and dispersion," *J. Fluid Mech.,* **42**, 49–60.
8. T.B. Benjamin and M.J. Lighthill, 1954, "On cnoidal waves and bores," *Proc. Roy. Soc. Lond. A,* **224**, 448–460.
9. D.R. Christie, 1989, "Long nonlinear waves in the lower atmosphere," *J. Atmos. Sci.,* **46**, 1462–1491.
10. A. Porter and N.F. Smyth, 2002, "Modelling the Morning Glory of the Gulf of Carpentaria," *J. Fluid Mech.,* **454**, 1–20.
11. P.G. Baines, 1995, *Topographic Effects in Stratified Flows,* Cambridge Monographs on Mechanics, Cambridge.
12. R.H.J. Grimshaw and N.F. Smyth, 1986, "Resonant flow of a stratified fluid over topography," *J. Fluid Mech.,* **169**, 429–464.
13. T.R. Marchant and N.F. Smyth, 1990, "The extended Korteweg-de Vries equation and the resonant flow of a fluid over topography," *J. Fluid Mech.,* **221**, 263–288.
14. N.F. Smyth, 1987, "Modulation theory solution for resonant flow over topography", *Proc. Roy. Soc. London A,* **409**, 79–97.
15. N.K. Lowman and M.A. Hoefer, 2013, "Dispersive shock waves in viscously deformable media," *J. Fluid. Mech.,* **718**, 524–557.
16. T.R. Marchant and N.F. Smyth, 2005, "Approximate solutions for magmon propagation from a reservoir," *IMA J. Appl. Math.,* **70**, 796–813.

17. G.A. El, A. Gammal, E.G. Khamis, R.A. Kraenkel and A.M. Kamchatnov, 2007, "Theory of optical dispersive shock waves in photorefractive media," *Phys. Rev. A,* **76**, 0523813.
18. M. Conforti, F. Baronio and S. Trillo, 2014, "Resonant radiation shed by dispersive shock waves," *Phys. Rev. A,* **89**, 013807.
19. M. Conforti and S. Trillo, 2014, "Radiative effects driven by shock waves in cavity-less four-wave mixing combs," *Opt. Lett.,* **39**, 5760–5763.
20. G.A. El and N.F. Smyth, 2016, "Radiating dispersive shock waves in non-local optical media," *Proc. Roy. Soc. London A,* **472**, 20150633.
21. N.F. Smyth, 2016, "Dispersive shock waves in nematic liquid crystals," *Physica D,* **333**, 301–309.
22. X. An, T.R. Marchant and N.F. Smyth, 2017, "Optical dispersive shock waves in defocusing colloidal media," *Physica D,* **342**, 45–56.
23. G.B. Whitham, 1965, "A general approach to linear and non-linear dispersive wave using a Lagrangian," *J. Fluid Mech.,* **22**, 273–283.
24. G.B. Whitham, 1965, "Non-linear dispersive waves," *Proc. Roy. Soc. London A,* **283**, 238–261.
25. B. Fornberg and G.B. Whitham, 1978, "Numerical and theoretical study of certain non-linear wave phenomena," *Phil. Trans. Roy. Soc. Lond. Ser. A,* **289**, 373–404.
26. A.V. Gurevich and L.P. Pitaevskii, 1974, "Nonstationary structure of a collisionless shock wave," *Sov. Phys. JETP,* **33**, 291–297.
27. G.A. El, V.V. Geogjaev, A.V. Gurevich and A.L. Krylov, 1995, "Decay of an initial discontinuity in the defocusing NLS hydrodynamics," *Physica D,* **87**, 186–192.
28. A.A. Minzoni and N.F. Smyth, 1997, "A modulation solutions of the signalling problem for the equation of self-induced transparency in the Sine-Gordon limit," *Math. Applic. Anal.,* **4**, 1–10.
29. A.M. Kamchatnov, Y.-H. Kuo, T.-C. Lin, T.-L. Horng, S.-C. Gou, R. Clift, G.A. El and R.H.J. Grimshaw, 2012, "Undular bore theory for the Gardner equation," *Phys. Rev. E,* **86**, 036605.
30. H. Flaschka, M.G. Forest and D.W. McLaughlin, 1980, "Multiphase averaging and the inverse spectral solution of the Korteweg-de Vries equation," *Comm. Pure Appl. Math.,* **33**, 739–784.
31. G.A. El, 2005, "Resolution of a shock in hyperbolic systems modified by weak dispersion," *Chaos,* **15**, 037103.
32. G.A. El, V.V. Khodorovskii and A.V. Tyurina, 2003, "Determination of boundaries of unsteady oscillatory zone in asymptotic solutions of non-integrable dispersive wave equations," *Phys. Lett. A,* **318**, 526–536.
33. M. Crosta, S. Trillo and A. Fratalocchi, 2012, "The Whitham approach to dispersive shocks in systems with cubic-quintic nonlinearities," *New J. Phys.,* **14**, 093019.
34. G.A. El, A.M. Kamchatnov, V.V. Khodorovskii, E.S. Annibale and A. Gammal, 2009, "Two-dimensional supersonic nonlinear Schrödinger flow past an extended obstacle," *Phys. Rev. E,* **80**, 046317.
35. G.A. El, L.T.K. Nguyen and N.F. Smyth, 2017, "Dispersive shock waves in systems with nonlocal dispersion of Benjamin-Ono type," *Nonlinearity,* submitted.
36. G.G. Stokes, 1880, "Supplement to a paper on the theory of oscillatory waves," *Math. Phys. Papers, Volume I,* Cambridge University Press, 314–326.
37. R.L. Seliger, 1968, "A note on the breaking of waves," *Proc. Roy. Soc. London A,* **303**, 493–496.
38. D. Moldabayev, H. Kalisch and D. Dutykh, 2015, "The Whitham equation as a model for surface water waves," *Physica D,* **309**, 99–107.
39. M. Ehrnström and H. Kalisch, 2009, "Traveling waves for the Whitham equation," *Diff. Int. Eqns.,* **22**, 1193–1210.
40. M. Ehrnström, M.D. Groves and E. Wahlén, 2012, "Solitary waves of the Whitham equation—a variational approach to a class of nonlocal evolution equations and existence of solitary waves of the Whitham equation," *Nonlinearity,* **25**, 2903–2936.
41. R.I. Joseph, 1977, "Solitary waves in a finite depth fluid," *Phys. A,* **10**, L225.
42. T.B. Benjamin, 1967, "Instability of periodic wavetrain in nonlinear dispersive systems," *Proc. Roy. Soc. Lond. A,* **299**, 59–76.
43. N. Sanford, K. Kodama, J.D. Carter and H. Kalisch, 2014, "Stability of traveling wave solutions to the Whitham equation," *Phys. Lett. A,* **378**, 2100–2107.
44. Y. Kodama, J. Satsuma and M.J. Ablowitz, 1981, "Nonlinear intermediate long-wave equation: analysis and method of solution," *Phys. Rev. Lett.,* **46**, 687–690 (1981).
45. A. Parker, 1992, "Periodic solutions of the intermediate long-wave equation: a nonlinear superposition principle," *J. Phys. A: Math. Gen.,* **25**, 2005-2032.
46. G.A. El, R.H.J. Grimshaw and W.K. Tiong, 2012, "Transformation of a shoaling undular bore," *J. Fluid Mech.,* **709**, 371-395.

47. G. El, R.H.J. Grimshaw and N.F. Smyth, 2006, "Unsteady undular bores in fully nonlinear shallow-water theory," *Phy. Fluids,* **18**, 027104.